molecular pharmaceutics

pubs.acs.org/molecularpharmaceutics

Article

Extracellular Vesicles Derived from Human Umbilical Cord MSC Improve Vascular Endothelial Function in In Vitro and In Vivo Models of Preeclampsia through Activating Arginine Metabolism

Zhaoer Yu,[§] Wei Zhang,[§] Yixiao Wang,[§] Mingming Gao, Min Zhang, Dan Yao, Chengping Qiao, Xianwei Cui,* and Ruizhe Jia*

Cite This: *Mol. Pharmaceutics* 2023, 20, 6429−6440

Read Online

ACCESS | Metrics & More | Article Recommendations | Supporting Information

ABSTRACT: Endothelial cell damage is an important feature of preeclampsia (PE). Human umbilical mesenchymal stem-cell-derived extracellular vesicles (HUMSCs-derived EVs) have been shown to have therapeutic effects on a variety of diseases and tissue damage. However, the therapeutic effect of HUMSCs-derived EVs on endothelial injury in PE remains unclear. This study explored the possible mechanism of HUMSCs-derived EVs in the treatment of endothelial cell injury. Tumor necrosis factor α- and lipopolysaccharide-induced endothelial dysfunction models were used to evaluate the therapeutic effect of HUMSCs-derived EVs on endothelial injury. We further constructed PE mouse models to explore the function of HUMSCs-derived EVs in vivo. The changes of metabolites in endothelial cells after HUMSCs-derived EVs treatment were analyzed by metabolomics analysis and further validated by cell experiments. HUMSCs-derived EVs treatment can alleviate endothelial cell injury in PE, involving cell proliferation, migration, angiogenesis, and anti-inflammatory. Importantly, administration of HUMSCs-derived EVs improves hypertension and proteinuria in PE mice, alleviates kidney damage, and promotes vascularization in the placenta. Furthermore, metabolomics analysis found that the arginine metabolic pathway is activated after HUMSCs-derived EVs treatment. We also observed increased arginine level, nitric oxide content, and nitric oxide synthase activity, and further experiments proved that activating the arginine metabolic pathway could alleviate endothelial dysfunction. Our results reveal that HUMSCs-derived EVs could ameliorate PE endothelial dysfunction by activating the arginine metabolic pathway and may serve as a therapeutic method for treating PE.

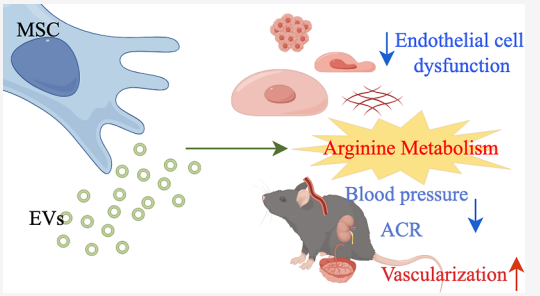

KEYWORDS: *mesenchymal stem cells, extracellular vesicles, preeclampsia, endothelial dysfunction, L-Arginine*

INTRODUCTION

Preeclampsia (PE) is a common hypertensive disorder of pregnancy characterized by a systemic vascular disorder. The diagnostic standard of PE is hypertension and proteinuria or without proteinuria but complicated with multiple organs and system dysfunction that appear after 20 weeks of pregnancy.[1] PE is one of the diseases with the highest maternal and fetal mortality, affecting an estimated 4 million women worldwide and causing the deaths of >70,000 women and 500,000 babies.[2] At present, there is still no effective drug treatment for PE. Pregnant women often need to terminate their pregnancy early. It is urgent to develop new treatment methods to improve maternal and infant outcomes.

Mesenchymal stem cells (MSCs) are a kind of cells with self-renewal ability and multidirectional differentiation potential, widely used in disease treatment and tissue damage repair research. MSC therapy can be used for the treatment of spinal cord injury,[3] autoimmune diseases,[4] diabetes mellitus,[5] acute respiratory distress syndrome,[6] and other diseases. Extracellular vesicles (EVs) are small particles with a bilayer lipid membrane structure released by living cells.[7] EVs have the advantages of low immunogenicity, low toxicity, and good biological tolerance. In comparison with live cell injection, EVs do not have the risk of uncontrollable behavior such as cell differentiation, and researchers have confirmed the safety of their intravenous application in animal experiments.[8] EVs derived from various cells have been studied for the treatment of diseases, such as necrosis of the femoral head,[9] chronic heart failure,[10] pulmonary fibrosis,[11] and ulcerative colitis.[12]

PE is a placenta-derived disease, and its development mainly includes two stages:[13] insufficient remodeling of uterine spiral arteries and systemic inflammatory damage. The first stage occurs in the placenta. Insufficient trophoblast invasiveness

Received: September 7, 2023
Revised: October 12, 2023
Accepted: October 16, 2023
Published: October 30, 2023

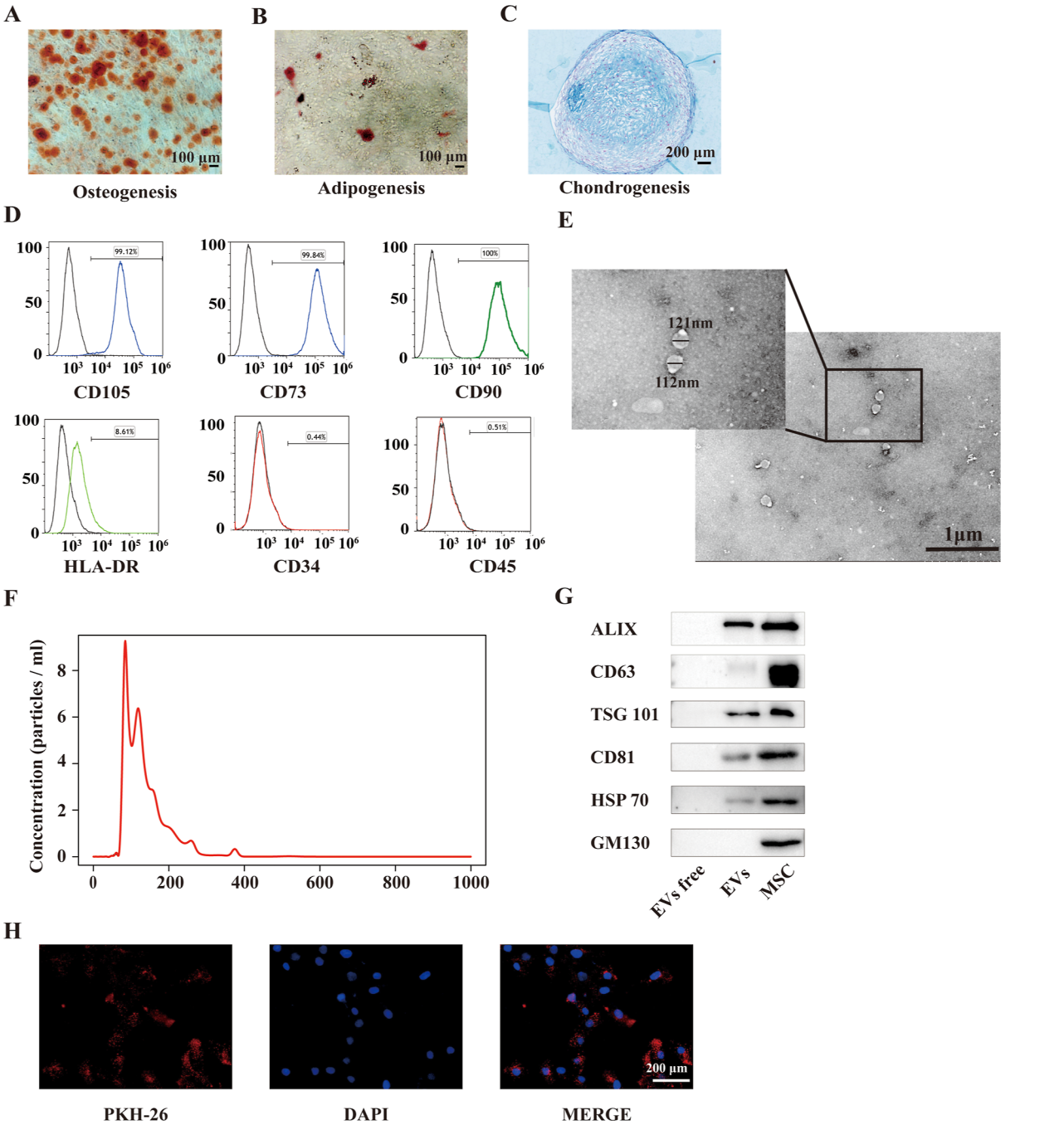

Figure 1. Identification of HUMSCs and HUMSCs-derived EVs. (A) Alizarin Red staining of calcium nodules in HUMSCs after osteogenic differentiation induction. (B) Oil Red O staining of lipid drops in HUMSCs after adipogenic differentiation induction. (C) Proteoglycan of chondrogenesis differentiation-induced HUMSCs was observed by Alcian blue staining. (D) Surface markers of HUMSCs were detected by flow cytometry analysis. The black line shows isotype control. (E) Transmission electron micrograph of HUMSCs-derived EVs. (F) NanoSight analysis of the particle size distribution of HUMSCs-derived EVs based on 5 experiments. (G) Detection of HUMSCs-derived EVs ALIX, CD63, TSG101, CD81, HSP70, and GM130 expression by Western blotting. (H) The PKH26-labeled EVs (red) were taken up by HUVECs. HUVECs nuclei were stained by DAPI.

leads to insufficient remodeling of the uterine spiral artery, abnormal placental perfusion, and placental dysfunction. This is the initial link in the pathogenesis of PE. The second stage is when PE manifests clinical symptoms. The dysfunctional placenta releases a variety of bioactive factors,[14] including a large number of antiangiogenic factors,[15] into the bloodstream. These bioactive molecules target vascular endothelial cells, resulting in extensive endothelial inflammation.[16] Eventually, the mother shows typical symptoms, such as hypertension and proteinuria. Therefore, improving vascular endothelial dysfunction is an important direction to explore the treatment of PE. However, the therapeutic effect of human umbilical mesenchymal stem cell-derived extracellular vesicles (HUMSCs-derived EVs) on endothelial injury in PE remains unclear.

This study aimed to explore the therapeutic effects of HUMSCs-derived EVs on PE in both endothelial cells and PE mice and to further reveal their potential mechanisms of action. Our exploration could help develop a potential PE treatment.

https://doi.org/10.1021/acs.molpharmaceut.3c00816
Mol. Pharmaceutics 2023, 20, 6429−6440

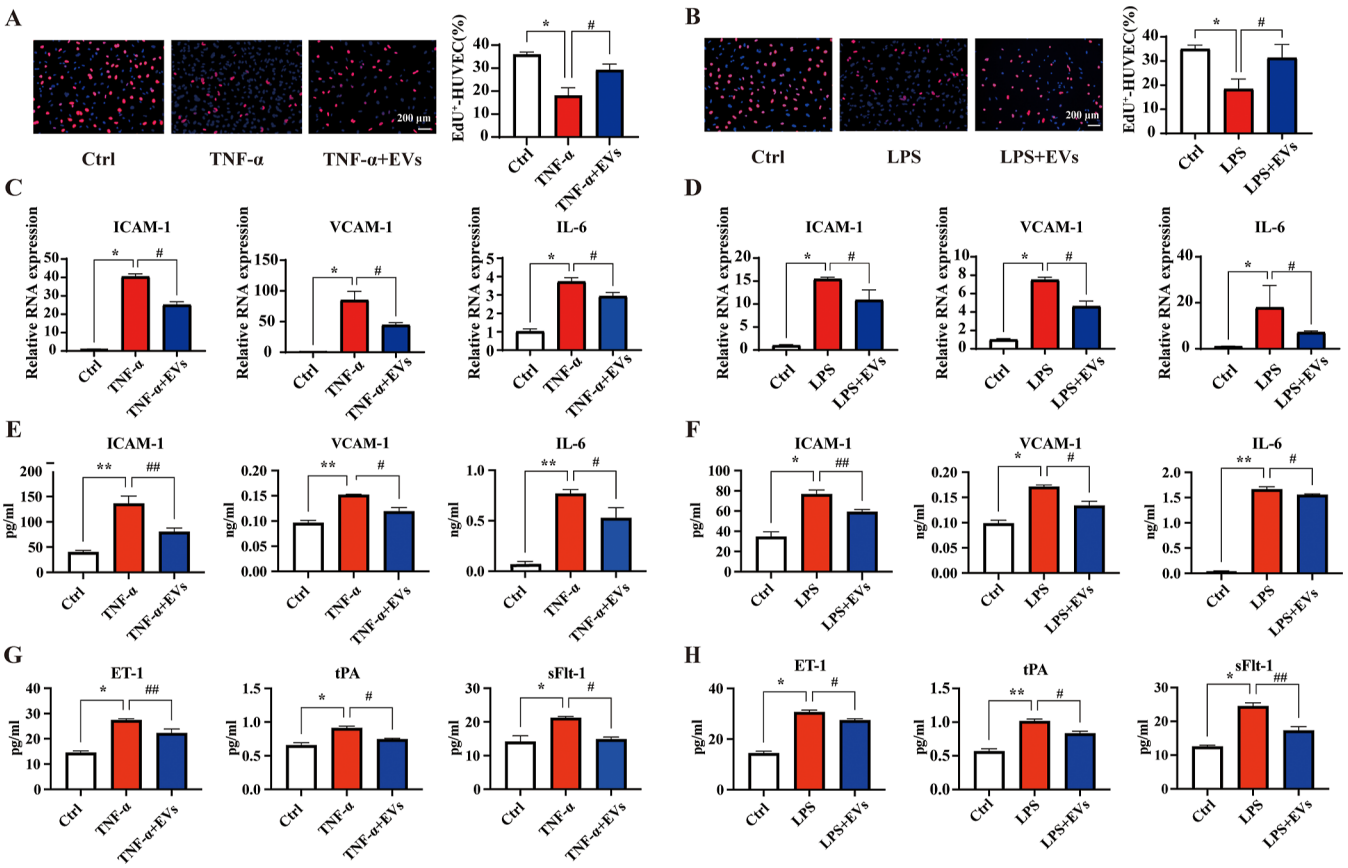

Figure 2. EVs ameliorate TNF-α or LPS-induced cell proliferation dysfunction and cell inflammation of HUVECs. (A,B) Cell proliferation of HUVECs stimulated with TNF-α/LPS or EVs together was detected by the EdU assay (EdU: red, DAPI: blue). EDU$^+$-HUVECs rates were analyzed statistically. (C,D) RT-qPCR detection of cellular inflammatory factors (ICAM-1, VCAM-1, and IL-6) mRNA expression of HUVECs stimulated with TNF-α/LPS or EVs together. (E,F) ELISA kit detected cellular inflammatory factors (ICAM-1, VCAM-1, and IL-6) expression of HUVECs of each group. (G,H) ELISA kit detected endothelial cell injury marker (ET-1, tPA and sFlt-1) expression of HUVECs of each group. $^*P < 0.05$, $^{**}P < 0.005$, $^{\#}P < 0.05$, and $^{\#\#}P < 0.005$.

MATERIALS AND METHODS

Ethics Statement. Ethical approval for this study for the acquisition of clinical specimens was obtained from the Ethics Committee of the Women's Hospital of Nanjing Medical University (2021KY-105). All animal experiments and procedures were approved by the Animal Core Facility of Nanjing Medical University (IACUC-2012054).

Cell Culture and Treatment. Samples of human umbilical cord were donated by donors who voluntarily delivered term babies by a cesarean section. Human umbilical cords were preserved and washed with PBS. Subsequently, human umbilical cord veins and arteries were removed and chopped into 1−2 mm pieces. Cord pieces were placed in a six-well plate and cultured in Dulbecco's modified Eagle's medium Nutrient Mixture F-12 (Ham) (DMEN/F12, Gibco, #11330500) supplemented with 10% fetal bovine serum (FBS) and 1% penicillin/streptomycin. The culture medium was changed every 3 d after the initial plating. HUMSCs were harvested and subcultured after reaching 80−90% confluence. For cryopreservation, HUMSCs were resuspended in a cryoprotectant solution consisting of 90% FBS and 10% dimethyl sulfoxide (DMSO) and stored in liquid nitrogen. In this study, HUMSCs between passages 3 and 7 were used for experiments.

Human umbilical vein endothelial cells (HUVECs) were purchased from ScienCell Research Laboratories and cultured in endothelial cell medium (ECM, ScienCell, #1001) at 37 °C with 5% CO_2. After HUVECs grew to 70% confluency, cells were treated with lipopolysaccharide (LPS) (1 μg/mL, Sigma, L2630), tumor necrosis factor-α (TNF-α)(20 ng/mL, Sigma, H8916), soluble FMS-like tyrosine kinase-1 (sFlt-1) (20 ng/mL, MedChemExpress, HY-P70636), EVs (50 μg/mL), or L-arginine (200 nM, Abmole, M6894) for 24 h in different experiments.

Identification of HUMSCs. P3 HUMSCs were digested and resuspended in PBS. Cells were then transferred to EP tubes at a concentration of 1×10^6/l00 μL. Each EP tube was added with labeled antibodies separately: FITC-CD90, FITC-HLA-DR, PE-CD45, PE-CD34, APC-CD105, APC-CD73, and isotype control antibodies (Biogems, USA). Cells were labeled for 15 min at room temperature, then washed with PBS and resuspended in 500 μL of PBS. There were at least 1×10^5 cells in each tube for detection using flow cytometry.

P3 HUMSCs were digested and inoculated in a 6-well plate. The culture medium was discarded and replaced with 2 mL of Osteogenic Differentiation Kit (STEMCELL Technologies, USA, #05465) or Adipogenic Differentiation Kit (STEMCELL Technologies, USA, #05412) after cell confluency reaching 90%. The culture medium was replaced every 3 days. After 20−30 days, cells were fixed with 4% polyoxymethylene and stained using 0.1% Alizarin Red S (Beyotime, China, no. C0148S) or Oil Red O (Beyotime, China, no. C0158S) for 20 min. The calcium nodules and lipid drops were observed and photographed under

https://doi.org/10.1021/acs.molpharmaceut.3c00816
Mol. Pharmaceutics 2023, 20, 6429−6440

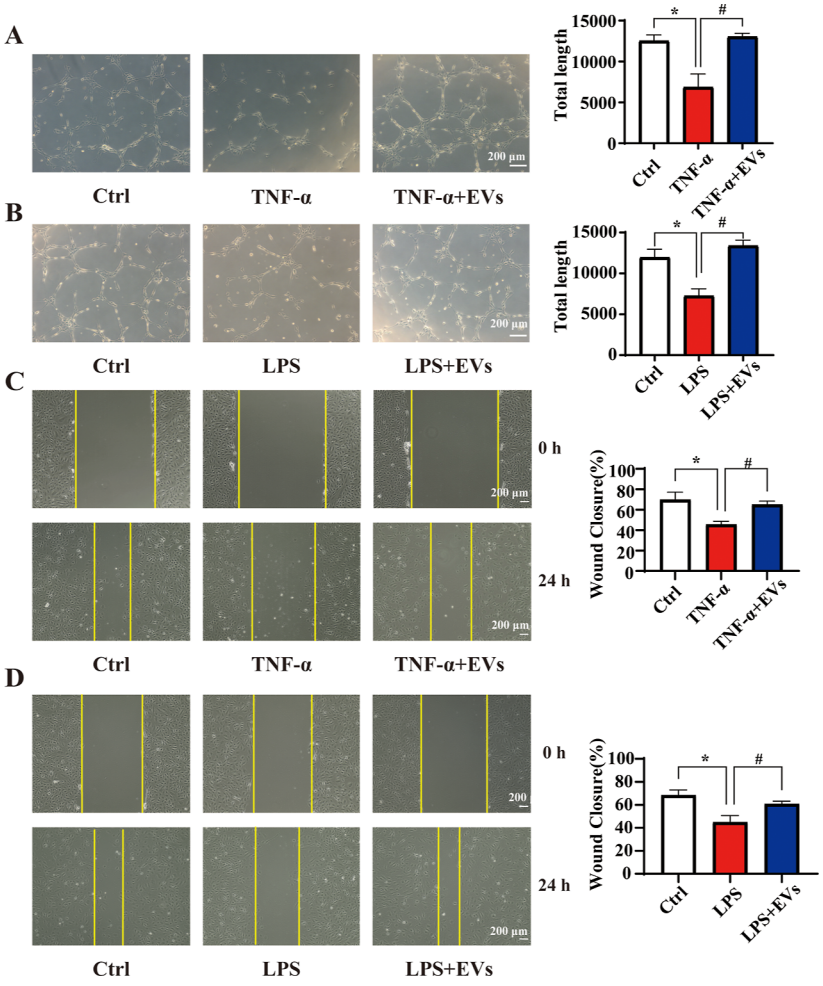

Figure 3. EVs ameliorate TNF-α or LPS-induced cell migration and angiogenesis dysfunction. (A,B) Angiogenesis ability of HUVECs under conditional treatment was determined by tube formation assay. Images were taken after 6 h. (C,D) Wound healing assay showed the changes of the migration ability of HUVECs. Images were taken after 24 h. $^{*}P < 0.05$ and $^{\#}P < 0.05$.

a microscope. 2×10^6 HUMSCs were resuspended in 2 mL of complete Chondrogenic Differentiation Medium (STEMCELL Technologies, USA, #05455), and 0.5 mL of the cell suspension was added to 15 mL polypropylene tubes. The cap of the tube was partially open and incubated for 3 days. 0.5 mL of complete chondrogenic differentiation medium was added to the tube and incubated for another 3 days. Half of it was replaced every 3 days up to day 21. The chondrogenic pellets was fixed in 10% formalin at room temperature for 30 min, following subsequent standard paraffin embedding methods and staining 6 μm sections with Alcian blue and Nuclear Fast Red.

Isolation and Identification of HUMSCs-derived EVs. HUMSCs between passages 3 and 7 were used for EVs isolation. FBS was centrifuged at 160,000*g* for 12 h at 4 °C to deplete EVs before HUMSCs culture. A medium of HUMSCs was collected after 48 h of culture in a complete medium containing 10% EV-depleted FBS. The collected medium was centrifuged at 500*g* for 15 min at room temperature to remove cells and subsequently centrifuged at 12,000*g* for 30 min at 4 °C to remove cell debris and apoptotic bodies. Then the supernatant was transferred to an ultracentrifuge tube (Beckman, USA) and centrifuged at 120,000*g* for 90 min at 4 °C to pellet EVs. EV pellets in each ultracentrifuge tube were resuspended in 100 μL of PBS and stored at −80 °C. The protein concentration of EVs was assayed by a BCA Protein Quantification Kit (Vazyme, China, E112-01). A transmission electron microscope (TEM) was used to observe the size and shape of the exosomes. Western blotting was used to determine the expressions of CD63 (1:1000, Abcam, ab134045), CD81 (1:1000, Abcam, ab109201), ALIX (1:1000, Abcam, ab275377), TSG101 (1:1000, Abcam, ab125011), HSP70 (1:1000, Abcam, ab181606), and GM130 (1:1000, Abcam, ab52649). NanoSight (NTA) was used to analyze the size of the EVs sample.

Uptake of HUMSCs-derived EVs. According to the manufacturer's instructions, EVs were labeled with the red fluorescent dye PKH26 kit (Sigma, USA, MINI26). HUVECs were coincubated with labeled HUMSCs-EVs for 24 h at 37 °C, washed 3 times with PBS to remove EVs that violate cellular uptake, and then fixed with 4% polyoxymethylene for 15 min. After washing with PBS again, the nuclei were stained with DAPI (Invitrogen, USA, #2188179). The signals were observed, and pictures taken with a fluorescence microscope.

Proliferation Assay. Cell proliferation was analyzed by a 5-ethynyl-2′-deoxyuridine (EdU) assay after treatment as described above. DNA synthesis was detected by Cell-Light EdU Apollo567 In Vitro Kit (Riobio, China, C10310-1) according to the manufacturer's instruction, and nuclei were stained with DAPI (Invitrogen, USA, #2188179) and photographed using a fluorescence microscope.

https://doi.org/10.1021/acs.molpharmaceut.3c00816
Mol. Pharmaceutics 2023, 20, 6429−6440

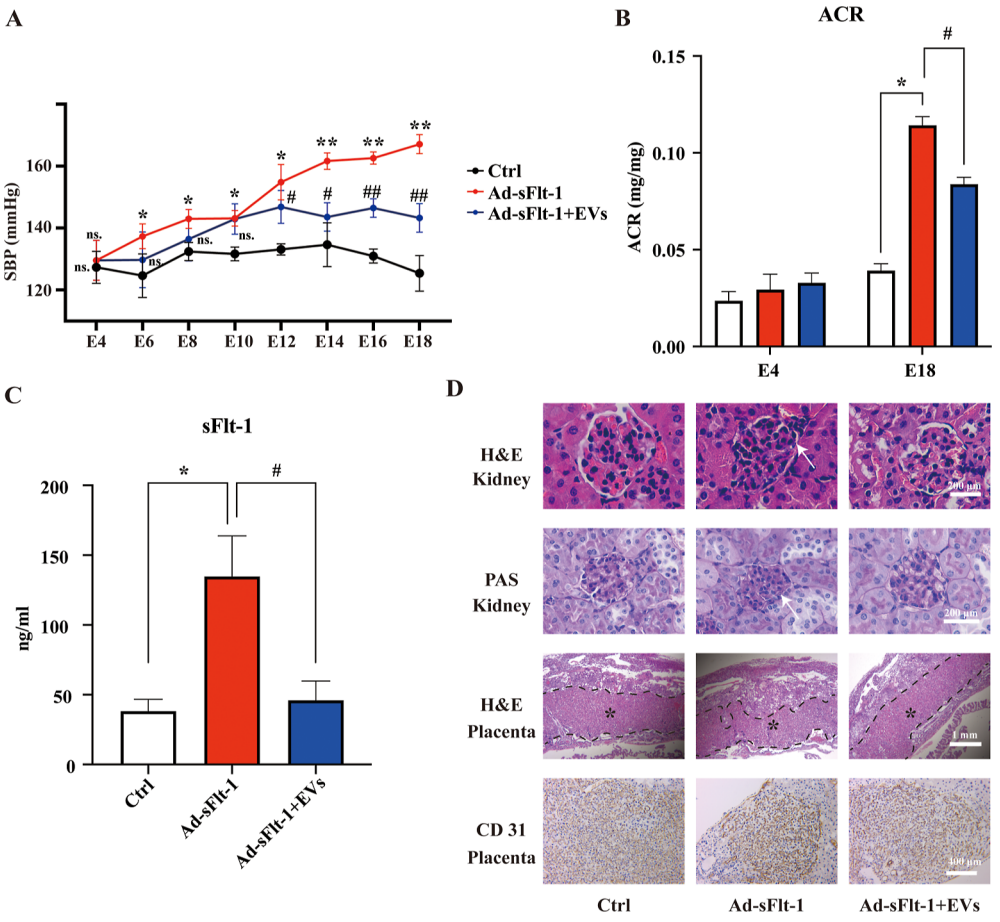

Figure 4. EVs improve symptoms in mice with PE (A) maternal tail-cuff blood pressure throughout gestation (n = 5). (B) Random urinary protein/creatinine ratio of maternal urine at E4 and E18. (C) ELISA analysis of maternal serum sFlt-1 at E18. (D) Representative H&E staining and PAS staining images of the mouse kidney from each group at E18; the arrows indicate renal glomeruli. H&E staining and CD31 immunohistochemistry of the mouse placenta from each group at E18; the asterisk indicate the placenta labyrinth zone. *P < 0.05, **P < 0.005, #P < 0.05, and ##P < 0.005.

Inflammation Factors Measurement. Inflammation factors of HUVECs were measured by reverse transcription quantitative PCR (RT-qPCR) and an ELISA Kit. For RT-qPCR, total RNA was extracted from HUVECs using the RNA Extraction Kit (Vazyme, China, RC101-01) according to the manufacturer's instructions. About 1 μg of RNA was reverse transcribed using the Hiscript III Reverse Transcriptase Kit (Vazyme, China, R302-01). qPCR was performed using the SYBR Green PCR master mix (Vazyme, China, Q712-02) using the StepOnePlus Real-Time PCR System (Thermo Fisher Scientific Inc., USA). Primer sequences are listed in Supporting Information Table 1. For the ELISA Kit, inflammation factors of HUVECs were measured according to the manufacturer's instructions, for example, human intercellular adhesion molecule 1 (ICAM-1) (EK1114, SAB), human vascular cell adhesion protein 1 (VCAM-1) (EK1368, SAB), and human interleukin-6 (IL-6) (EK1217, SAB).

Endothelial Cell Injury Marker Measurement. Endothelial cell injury markers of HUVECs were measured according to the manufacturer's instructions, including human endothelin-1 (ET-1) (EK1832, SAB), human tissue-type plasminogen activator (tPA) (EK1870, SAB), and human vascular endothelial growth factor receptor 1 (ELISA Kit, EK1384, SAB).

Tube Formation Assay. 200 μL cold Matrigel Matrix (Corning, USA, #354248) per well was transferred into a 24-well plate and incubated at 37 °C for 2 h. Then, HUVECs (1×10^5 cells per well) were seeded into the Matrigel-coated 24-well plates and treated as described above. 6−8 h after seeding, an inverted microscope was used to detect the tube formation. The total length of the tubes was measured by ImageJ software.

Wound Healing Assay. HUVECs were seeded in a six-well plate and cultured in ECM 5% FBS. When cells reached confluence, cells were treated with mitomycin C (10 μg/mL, Abmole, China, #M5791) for 2 h. The mitomycin C treated cells were extensively washed in PBS, and a scratch wound was created across each well using a 200 μL pipet tip. Then cells were cultured in ECM with 1% FBS and treated differently as described above for another 24 h. The migration of cells into the "wound closure" was photographed and measured by ImageJ software. The following formula calculated the rate of migration: wound closure (%) = $(A_0 - A_n)/A_0 \times 100$, A_0 represents the initial wound area, and A_n represents the remaining wound area after 24 h.

Animal Experiments. C57BL/6J mice were obtained at 8−10 weeks weighing 25−30 g from the Beijing Vital River Laboratory Animal Technology Co., Ltd. The mice were housed under specific pathogen-free conditions with a 12 h light/12 h dark cycle at the Animal Core Facility of Nanjing Medical University. After 1 week of feeding to adapt the environment, female and male mice were kept in the same cage at a ratio of 2:1. The cohabitation was from 16:00 to 8:00 the next day. After the mice were separated, the vaginal plug was checked. Mice with

https://doi.org/10.1021/acs.molpharmaceut.3c00816
Mol. Pharmaceutics 2023, 20, 6429−6440

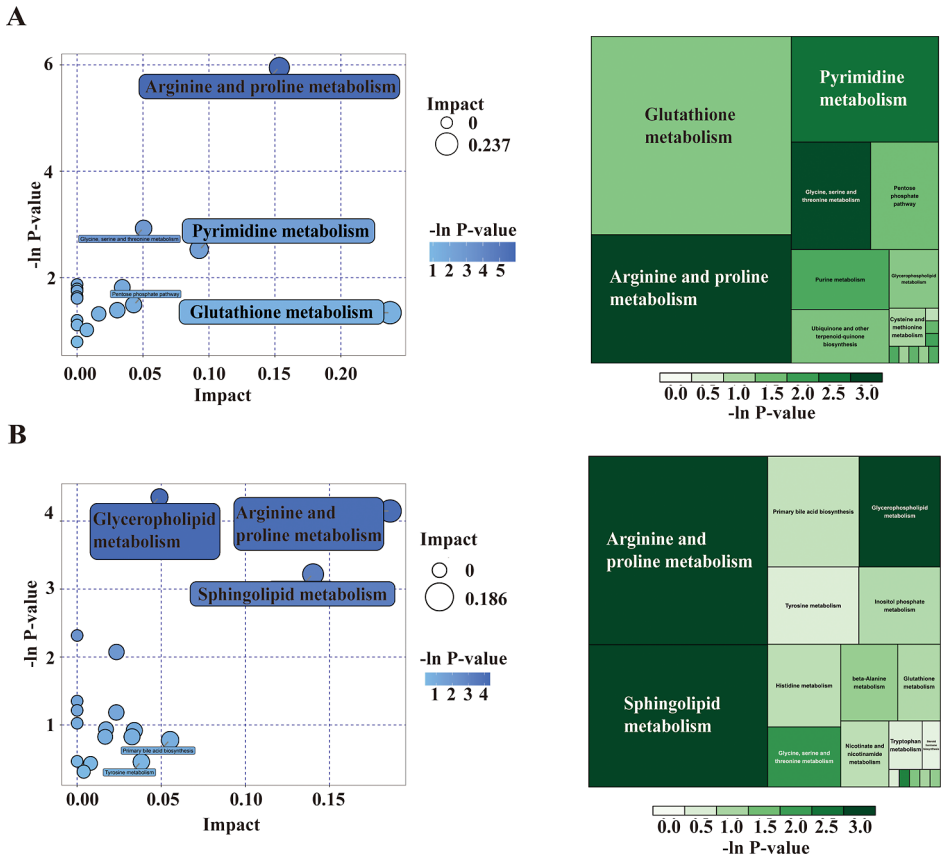

Figure 5. EVs alleviate endothelial dysfunction associated with L-arginine metabolism. (A) Plotted map and tree map showed the different metabolisms of HUVECs after EVs were cocultured and analyzed by KEEG pathway analysis. (B) Plotted map and tree map show the metabolism of EVs analyzed by KEEG pathway analysis.

vaginal plugs detected were considered 0.5 days pregnant (E0.5). The pregnant mice were randomly grouped into three groups (5 for each group): control group (tail vein injection of control adenovirus on E5.5), PE group (tail vein injection of sFlt-1 adenovirus on E5.5), and EVs treatment group (tail vein injection of sFlt-1 adenovirus on the E5.5 and tail vein injection of HUMSCs-EVs 100 μg/mouse/day on E6.5 to E18.5). Blood pressure was monitored every other day from E4.5 to E18.5 using the noninvasive tail artery blood pressure measurement and analysis system. Random urine samples were collected on E4.5 and E18.5, urine protein was detected by the Albuwell M (Mouse Albumin ELISA) Kit (Exocell, USA, #1011), and urine creatine was detected by the Creatinine Assay kit (Nanjing Jiancheng Bioengineering Institute, China, #011-2-1). Urinary albumin/creatinine ratio (ACR) was calculated by the following formula: ACR = urine creatine/urine protein. At E18.5, the mice were anesthetized with highly concentrated isoflurane in CO_2 (approximately 60% inhalation) to collect blood, kidney, and placenta. Plasma sFlt-1 was detected by the mouse Flt-1 Quantikine ELISA Kit (R&D, USA, MVR100). The histological assessment included the evaluation of placental and kidney biopsy specimens. Hematoxylin and eosin stain (H&E) and periodic acid Schiff (PAS) staining of the kidney were used to assess glomerular damage. H&E staining and immunohistochemistry against CD31 (Abcam, USA, ab182981) of the placenta was used to determine labyrinth and vascularization.

Metabolomics Analysis. LC−MS/MS analyses were performed using a UHPLC system (Vanquish, Thermo Fisher Scientific) by the Biotree Biomedical Technology Company in Shanghai. The UPLC BEH Amide column (2.1 × 100 mm, 1.7 μm) was coupled to an Orbitrap Exploris 120 mass spectrometer (Orbitrap MS, Thermo). The mobile phase consisted of component A [25 mmol/L ammonium acetate and 25 ammonia hydroxide in water (pH = 9.75)] and component B (acetonitrile). The autosampler temperature was set to 4 °C and the injection volume to 2 μL. MS/MS spectra were acquired in information-dependent acquisition mode in the control of the acquisition software (Xcalibur, Thermo) by The Orbitrap Exploris 120 mass spectrometer. In this mode, the full scan MS spectrum is evaluated by the acquisition software continuously. The ESI source conditions were set as follows respectively: Aux gas flow rate as 15 Arb, sheath gas flow rate as 50 Arb, full MS resolution as 60,000, capillary temperature at 320 °C, MS/MS resolution as 15,000 collision energy as 10/30/60 in NCE mode, spray voltage as 3.8 kV (positive) or −3.4 kV (negative). The raw data were converted to the mzXML format using ProteoWizard and processed using an in-house program developed in R and based on XCMS for peak detection, extraction, alignment, and integration. Metabolite annotation was performed by using the in-house MS2 database (BiotreeDB). The cutoff value for annotation was set to 0.3.

For metabolic pathway enrichment analysis of differential metabolites, we mapped metabolite databases such as Kyoto Encyclopedia of Genes and Genomes (KEGG) and PubChem by differential metabolites and then searched and analyzed the metabolic pathway of the pathway database of the corresponding species, *Homo sapiens* (human). The results of the metabolic

https://doi.org/10.1021/acs.molpharmaceut.3c00816
Mol. Pharmaceutics 2023, 20, 6429−6440

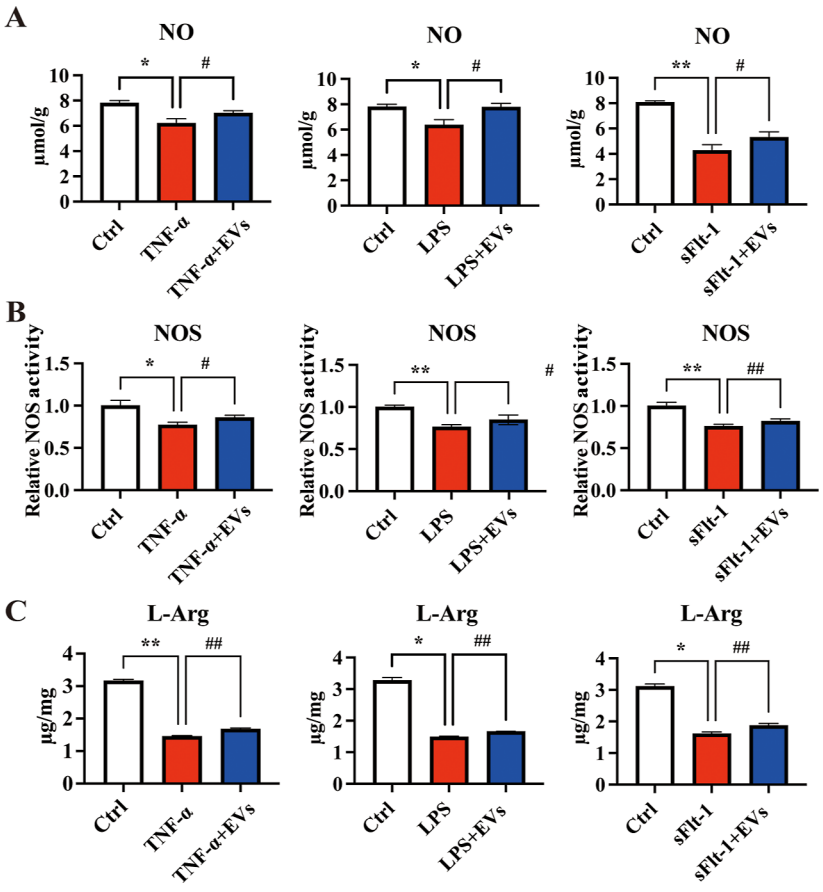

Figure 6. EVs active arginine metabolism in vitro. (A) Intracellular NO level of HUVECs after TNF-α, LPS, or sFlt-1 treated with or without EVs cocultured (standardized by the total protein content of cells). (B) Relative intracellular NOS activity of each group. (C) Intracellular L-arginine levels of each group (standardized by the total protein content of cells). *$P < 0.05$, **$P < 0.005$, $^{\#}P < 0.05$, and $^{\#\#}P < 0.005$.

pathway analysis are displayed in a bubble plot and a tree map plot.

Nitric Oxide (NO) and L-Arginine Measurement. HUVECs were lysed in ice-cold lysis buffer for the NO assay (Beyotime Biotechnology, China, S3090), and Intracellular NO production was determined by the Nitrate/Nitrite Assay Kit (Beyotime Biotechnology, China, S0023) as per the manufacturer's instructions. The intracellular L-arginine in HUVECs cell lysis was determined by the ELISA Kit (Cloud-Clone Corp., CEB938Ge) as per the manufacturer's instructions.

Endothelial Nitric Oxide Synthase (NOS) Activity Assay. Intracellular NOS activity in HUVECs cell lysis was determined by the total nitric oxide synthase assay kit (Nanjing Jiancheng Bioengineering Institute, China, #A104-2-2) as per the manufacturer's instructions.

Statistical Analysis. All data were statistically analyzed and graphed by GraphPad Prism 9 (San Diego, CA, United States). Measurement data were expressed as the mean ± standard deviation. Each experiment was repeated at least three times. Student's *t*-test was used to compare the variation between the two groups. Using one-way analysis of variance (ANOVA) was used to compare variation among three groups, after which pairwise comparison was performed with Tukey's multiple comparisons test. $P < 0.05$ demonstrated a statistically significant difference.

RESULTS

Isolation and Identification of HUMSCs and HUMSCs-derived EVs. The HUMSCs were isolated and cultured by the method of tissue block adhesion. To detect the differentiation potential of isolated HUMSCs, calcium nodules were observed with Alizarin Red S staining after Osteogenic induction (Figure 1A). Lipid drops were observed with Oil Red O staining after adipogenic induction (Figure 1B). Alcian blue staining was used to assess the chondrogenic differentiation of the HUMSCs (Figure 1C). Additionally, the expression of surface markers in cultured HUMSCs was detected by flow cytometry analysis, and the results showed that CD105, CD73, and CD90 on the cell surface were positive while HLA-DR, CD34, and CD45 were negative (Figure 1D). All these results indicate the multipotency of HUMSCs.

EVs were harvested from HUMSCs culture media using ultracentrifugation and characterized by NTA, TEM, and Western blot. NanoSight analysis showed the particle size distribution of HUMSCs-derived EVs was from 100 to 200 nm based on 5 experiments (Figure 1F). By TEM, it was also found that HUMSCs-derived EVs were small round particles with diameters of 100−200 nm (Figure 1E). Western blot showed that EV protein markers ALIX, CD63, TSG101, CD81, and HSP70 were all positively expressed in the samples, but GM130 was negatively expressed (Figure 1G). The red fluorescent dye PKH26 labeled EVs was used to observe the HUVECs uptaking EVs. After 24 h of incubation, the red fluorescent signal was observed by the fluorescence microscope to gather around the

https://doi.org/10.1021/acs.molpharmaceut.3c00816
Mol. Pharmaceutics 2023, 20, 6429−6440

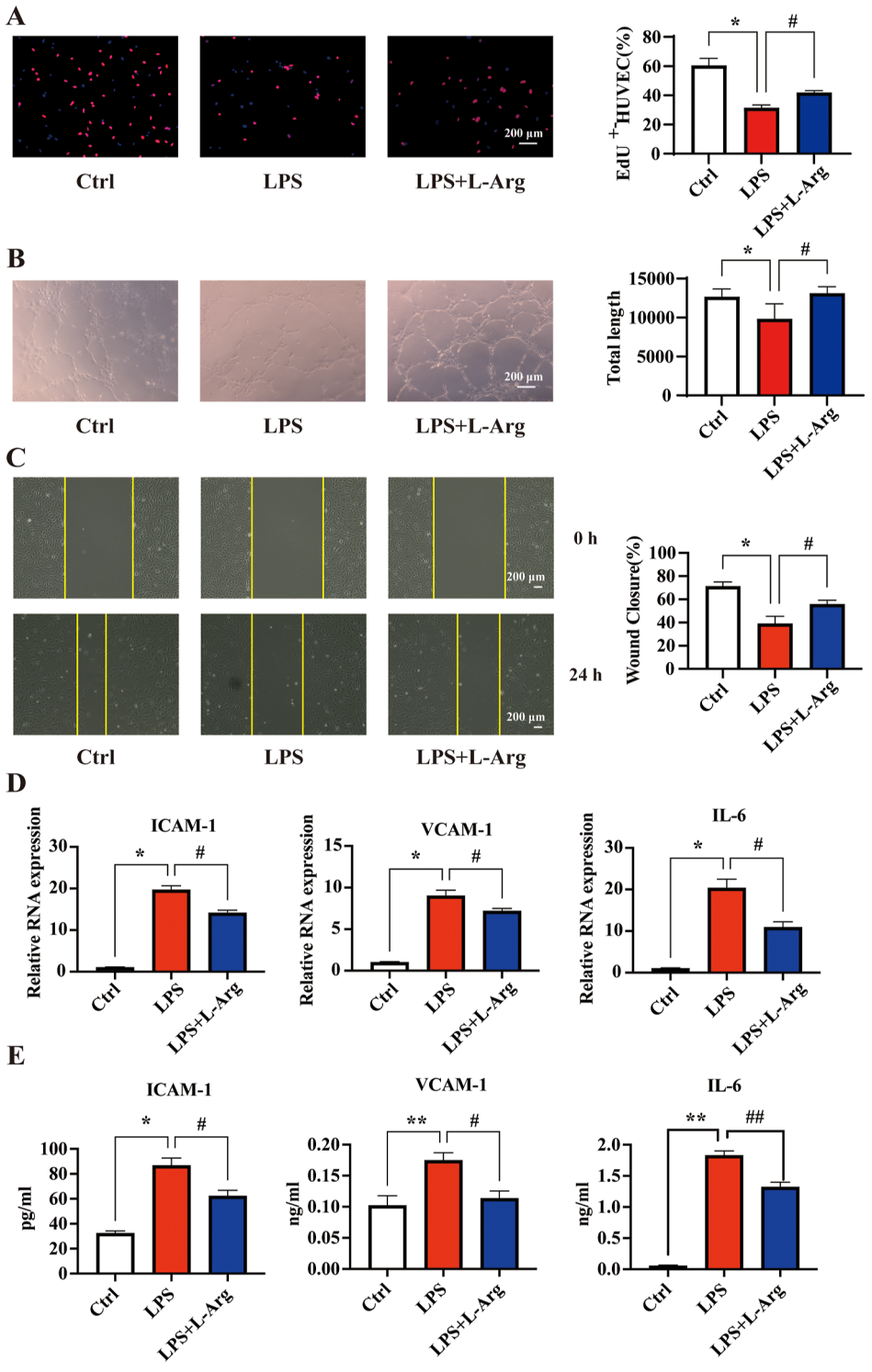

Figure 7. Arginine treatment ameliorates LPS-induced endothelial dysfunction. (A) Cell proliferation of HUVECs of each group was detected by the EdU assay (EdU: red, DAPI: blue). EDU^{+}-HUVECs rates were analyzed statistically. (B) Angiogenesis ability of HUVECs of each group was determined by tube formation assay. Images were taken after 6 h. (C) Wound healing assay showed the migration ability of HUVECs of each group. Images were taken after 24 h. (D) RT-qPCR detection of cellular inflammatory factors (ICAM-1, VCAM-1, and IL-6) mRNA expression of HUVECs of each group. (E) ELISA Kit detected cellular inflammatory factors (ICAM-1, VCAM-1, and IL-6) expression of HUVECs of each group. $^{*}P < 0.05$, $^{**}P < 0.005$, $^{\#}P < 0.05$, and $^{\#\#}P < 0.005$.

nucleus of endothelial cells, indicating that the EVs entered into the cells successfully (Figure 1H).

EVs Ameliorate TNF-α or LPS-induced Endothelial Cell Dysfunction. To mimic endothelial cell injury in PE patients, we induced dysfunction of HUVECs with TNF-α or LPS. The endothelial cell's proliferative ability, migration ability, and angiogenesis ability in vitro decreased after TNF-α or LPS treatment, while expression of inflammatory factors (ICAM-1, VCAM-1, and IL-6) and endothelial cell injury marker (ET-1, tPA, and sFlt-1) increased. After coculturing with EVs,

https://doi.org/10.1021/acs.molpharmaceut.3c00816
Mol. Pharmaceutics 2023, 20, 6429−6440

endothelial dysfunction was found to be alleviated. EVs could promote cell proliferation (Figure 2A,B) and reduce inflammatory factor (Figure 2C−F) and endothelial cell injury marker expression (Figure 2G,H) in the PE endothelial cell dysfunction model. In the wound healing assay and tubule formation assay, EV also showed good effects on promoting angiogenesis (Figure 3A,B) and cell migration (Figure 3C,D) in vitro.

EVs Improve Symptoms in Mice with PE. The PE mouse model was constructed by tail vein sFlt-1 adenovirus injection at E5. In comparison with PE mice, EVs treatment partially alleviated hypertensive symptoms (Figure 4A), decreased ACR at the end of pregnancy (Figure 4B), and reduced circulating sFlt-1 levels (Figure 4C). H&E and PAS staining of mouse kidneys showed that the renal glomerular capillaries of PE group mice were occluded and endothelial cells proliferated. While the EVs treatment can ameliorate kidney and placental damage (Figure 4D). CD31 is a classic vascular endothelial cell marker, and immunohistochemical results showed that the placenta of PE mice lacked vascularization, while the labyrinthine sinusoids were more abundant after EVs treatment (Figure 4D).

EVs Alleviate Endothelial Dysfunction Associated with L-Arginine Metabolism. Metabolites in EVs cocultured endothelial cell samples and EVs samples were analyzed using metabolomic methods, and KEEG pathway analysis was performed. The results showed that compared with normal cultured endothelial cells, the arginine and proline metabolic pathways of endothelial cells treated with EVs were activated, and arginine and other substances significantly related to this metabolic pathway could also be detected in EVs samples (Figure 5A,B).

EVs Active Arginine Metabolism In Vitro. To verify the effect of EVs on arginine metabolism, we detected the changes of L-arginine level, NOS activity, and NO level in cells after EVs treatment in PE endothelial cell dysfunction models. The results showed that arginine metabolism was activated in HUVECs cocultured with EVs, and intracellular NO levels (Figure 6A), NOS activity (Figure 6B), and L-arginine levels (Figure 6C) were significantly increased.

L-Arginine Treatment Ameliorates LPS-induced Endothelial Dysfunction. To further explore the effect of L-arginine on endothelial dysfunction in PE, we used the LPS-induced endothelial dysfunction model again to examine the effect of L-arginine; the proliferation, angiogenesis, migration ability, and the expression of inflammatory factors of endothelial cells were detected, including the intracellular NOS activity and the NO level. We determined that L-arginine treatment promoted cell proliferation (Figure 7A), angiogenesis in vitro (Figure 7B), cell migration (Figure 7C), and reduced expression of inflammatory factors (Figure 7D).

DISCUSSION

Our study demonstrated that HUMSCs-derived EVs can alleviate endothelial cell dysfunction. In vitro experiments showed that HUMSCs-derived EVs could promote endothelial cell proliferation, migration, and angiogenesis and reduce cellular inflammatory damage. In 1989, Robert and co-workers proposed that PE is an endothelial cell disease rather than pure hypertension, and the impaired coagulation and vasoconstriction function of endothelial cells leads to the development of hypertension.[17] During the development of PE, a variety of endothelial cell dysfunctions can be observed, such as decreased proliferation, migration, and angiogenesis ability,[18] cellular inflammatory response, oxidative stress,[19] and vasoconstriction dysfunction.[20] Researchers have found that relieving endothelial cell dysfunction through various means can treat PE, such as Priscila Rezeck Nunes using glyburide to enhance the antioxidant capacity of endothelial cell.[21] Liu et al. uses procyanidin B2 to attenuate sFlt-1-induced endothelial dysfunction and impaired angiogenesis,[22] Gu et al. uses esomeprazole to inhibit hypoxia/endothelial dysfunction-induced autophagy in PE.[23] Previous researchers have confirmed that endothelial cells are an effective target for the treatment of PE. Our study also shows that HUMSCs-derived EVs, as an excellent damage repair drug, can effectively alleviate endothelial cell dysfunction and have the potential to treat PE.

In vivo experiments, we used the intravenous injection of an sFlt-overexpressing adenovirus to construct a PE mouse model. HUMSCs-derived EVs can ameliorate the symptoms of sFlt-overexpressing adenovirus-induced PE in mice, alleviate kidney damage, and increase the vascularization of the placental labyrinth. sFlt-1 is an important antiangiogenic factor that can competitively bind to vascular endothelial growth factor (VEGF) and placental growth factor (PlGF) in circulation and antagonize the angiogenesis effect of VEGF and PlGF. The maternal placenta releases large amounts of sFlt-1 into the blood during PE development,[24] inducing endothelial cell dysfunction. We found that MSC-derived EVs treatment can improve PE symptoms such as hypertension and proteinuria, promote vascularization of the labyrinth in the placenta, and significantly reduce the concentration of sFlt-1 in serum.

Previous studies have shown that MSC-derived EVs can protect trophoblasts or endothelial cells through the transmission of microRNA (miRNA), long noncoding RNA (lncRNA), and other mechanisms.[25,26] To further explore the possible mechanism by which EVs improve vascular endothelial dysfunction, we used metabolomics analysis to compare the changes of metabolites in endothelial cells after EV treatment and performed a KEEG pathway analysis of the differential metabolites. It was found that the metabolism of arginine and proline in cells was significantly changed after the EV treatment. Metabolomic analysis of EV samples also found that the metabolites in EVs were significantly related to arginine and proline metabolism, and substances such as L-arginine were detected in the EV samples. L-arginine is an immediate precursor of NO, considering the important role of NO in regulating vasodilation, and many studies have attempted to improve perinatal outcomes in hypertensive disorder-complicating pregnancy by supplementation with L-arginine and reported positive results. As recently reviewed by Menichini et al.,[27] L-arginine supplementation reduces the development of PE and lowers blood pressure. In pregnant women with fetal growth restriction, L-arginine contributes to an increased birth weight, improved placental circulation, and neonatal outcomes. In our study, we treated the endothelial cell injury model with L-arginine alone and determined that L-arginine can promote endothelial cell proliferation, migration, and angiogenesis in vitro and inhibit inflammation.

EVs are loaded with abundant cargoes such as RNA, DNA, proteins, and small molecular compounds. Abundant miRNAs in EVs have been shown to play important roles in endothelial cells function, such as regulating angiogenesis,[25] inflammatory responses,[28] and cytokine production.[29] Metabolites in EVs, such as L-arginine, also have therapeutic effects on endothelial cell dysfunction. L-arginine is a substrate for intracellular NO generation and can be directly catalyzed by NOS to generate NO. As a signal transduction agent, NO is involved in many

https://doi.org/10.1021/acs.molpharmaceut.3c00816
Mol. Pharmaceutics 2023, 20, 6429−6440

basic life activities, such as the regulation of vasodilation, blood pressure regulation, and inflammatory response. During pregnancy, NO mainly affects vasodilation, regulation of blood volume, placental remodeling, and VEGF synthesis.[30] Studies on NO levels in PE patients have conflicting results, but more studies report lower serum NO levels in PE patients,[31] and using NOS inhibitors NG-nitro-L-arginine methyl ester (L-NAME) can induce PE symptoms in pregnant rats.[32] In the process of PE, NO synthesis is inhibited by many ways,[33] including increased arginase activity which depletes the substrate L-arginine, increased levels of asym-dimethylarginine (ADMA),[34] the competitive inhibitor of L-arginine, and reduced endothelial NOS activity after glutathionylation[35] or 4-oxo-2(*E*)-nonenal (ONE) modification.[36] In our study, EVs could promote NO synthesis by upregulating the NOS activity and increasing intracellular L-arginine levels, which may be one of the mechanisms by which EVs improve endothelial cell dysfunction. However, the regulation of NO biosynthesis is complex and diverse; the effect of EVs on arginase or ADMA still needs to be further explored, and the specific mechanism of NOS activity regulation is still unclear.

One of the limitations of this study is that the use of a single animal model, sFlt-1, overexpressing adenovirus-induced PE in mice cannot perfectly mimic the pathological state of PE. In addition, our study cannot rule out the effects of nucleic acids and proteins carried by EVs on endothelial cells. The potential mechanisms of these substances remain to be further explored.

CONCLUSIONS

MSC-derived EVs can improve vascular endothelial injury in PE by regulating arginine metabolism and NO synthesis, promoting endothelial cell proliferation and angiogenesis in vitro and improving symptoms in PE model mice. Our study demonstrates EVs as a potential approach for PE treatment.

ASSOCIATED CONTENT

Supporting Information

The Supporting Information is available free of charge at https://pubs.acs.org/doi/10.1021/acs.molpharmaceut.3c00816.

Primer sequences (PDF)

AUTHOR INFORMATION

Corresponding Authors

Xianwei Cui − *Nanjing Maternal and Child Health Institute, Women's Hospital of Nanjing Medical University, Nanjing Maternity and Child Health Care Hospital, Nanjing 210004, China*; Email: xwcui@njmu.edu.cn

Ruizhe Jia − *Department of Obstetrics and Gynecology and Nanjing Maternal and Child Health Institute, Women's Hospital of Nanjing Medical University, Nanjing Maternity and Child Health Care Hospital, Nanjing 210004, China*; orcid.org/0000-0002-3838-165X; Email: jiaruizhe2016@163.com

Authors

Zhaoer Yu − *Department of Obstetrics and Gynecology and Nanjing Maternal and Child Health Institute, Women's Hospital of Nanjing Medical University, Nanjing Maternity and Child Health Care Hospital, Nanjing 210004, China*

Wei Zhang − *Department of Obstetrics and Gynecology and Nanjing Maternal and Child Health Institute, Women's Hospital of Nanjing Medical University, Nanjing Maternity and Child Health Care Hospital, Nanjing 210004, China*

Yixiao Wang − *Department of Obstetrics and Gynecology, Women's Hospital of Nanjing Medical University, Nanjing Maternity and Child Health Care Hospital, Nanjing 210004, China*

Mingming Gao − *Department of Obstetrics and Gynecology, Women's Hospital of Nanjing Medical University, Nanjing Maternity and Child Health Care Hospital, Nanjing 210004, China*

Min Zhang − *Nanjing Maternal and Child Health Institute, Women's Hospital of Nanjing Medical University, Nanjing Maternity and Child Health Care Hospital, Nanjing 210004, China*

Dan Yao − *Department of Obstetrics and Gynecology, Women's Hospital of Nanjing Medical University, Nanjing Maternity and Child Health Care Hospital, Nanjing 210004, China*

Chengping Qiao − *Department of Obstetrics and Gynecology, Women's Hospital of Nanjing Medical University, Nanjing Maternity and Child Health Care Hospital, Nanjing 210004, China*

Complete contact information is available at: https://pubs.acs.org/10.1021/acs.molpharmaceut.3c00816

Author Contributions

[§]Z.Y., W.Z., and Y.W. authors contributed equally to this work. Z.Y., W.Z., and Y.W. carried out the experiments and drafted the manuscript, M.G. participated in the design of the study, D.Y. participated in the statistical analysis, C.Q. carried out the acquisition of clinical specimens, X.C. and R.J. conceived of the study, and participated in its design and coordination and helped to draft the manuscript. All authors read and approved the final manuscript.

Funding

This study was supported by grants from the National Natural Science Foundation of China (no. 81971393).

Notes

The authors declare no competing financial interest.

ACKNOWLEDGMENTS

We thank Figdraw (www.figdraw.com) for its help in creating Table of Content.

LIST OF ABBREVIATIONS

PE, preeclampsia; HUMSCs, human umbilical mesenchymal stem cells; EVs, extracellular vesicles; HUVECs, human umbilical vein endothelial cells; ECM, endothelial cell medium; FBS, fetal bovine serum; LPS, lipopolysaccharide; TNF-α, tumor necrosis factor-α; sFlt-1, soluble FMS-like tyrosine kinase-1; TEM, transmission electron microscope; NTA, NanoSight; EdU, 5-ethynyl-2′-deoxyuridine; ICAM-1, intercellular adhesion molecule-1; VCAM-1, vascular cell adhesion protein-1; IL-6, interleukin-6; ET-1, endothelin-1; tPA, tissue-type plasminogen activator; ACR, albumin/creatinine ratio; H&E, hematoxylin and eosin stain; PAS, periodic acid Schiff; NO, nitric oxide; NOS, nitric oxide synthase; miRNA, microRNA; lncRNA, long noncoding RNA; L-NAME, NG-nitro-L-arginine methyl ester; ADMA, asym-dimethylarginine

REFERENCES

(1) Gestational Hypertension and Preeclampsia: ACOG Practice Bulletin Summary, Number 222. *Obstet. Gynecol.* **2020**, *135* (6), 1492−1495,

(2) Dimitriadis, E.; Rolnik, D. L.; Zhou, W.; Estrada-Gutierrez, G.; Koga, K.; Francisco, R. P. V.; Whitehead, C.; Hyett, J.; da Silva Costa, F.; Nicolaides, K.; et al. Pre-eclampsia. *Nat. Rev. Dis. Prim.* **2023**, *9* (1), 8.

(3) Li, L.; Xiao, B.; Mu, J.; Zhang, Y.; Zhang, C.; Cao, H.; Chen, R.; Patra, H. K.; Yang, B.; Feng, S.; et al. A MnO_2 Nanoparticle-Dotted Hydrogel Promotes Spinal Cord Repair via Regulating Reactive Oxygen Species Microenvironment and Synergizing with Mesenchymal Stem Cells. *ACS Nano* **2019**, *13* (12), 14283−14293.

(4) Chen, Y.; Yu, Q.; Hu, Y.; Shi, Y. Current Research and Use of Mesenchymal Stem Cells in the Therapy of Autoimmune Diseases. *Curr. Stem Cell Res. Ther.* **2019**, *14* (7), 579−582.

(5) Päth, G.; Perakakis, N.; Mantzoros, C. S.; Seufert, J. Stem cells in the treatment of diabetes mellitus - Focus on mesenchymal stem cells. *Metabolism* **2019**, *90*, 1−15.

(6) Lanzoni, G.; Linetsky, E.; Correa, D.; Messinger Cayetano, S.; Alvarez, R. A.; Kouroupis, D.; Alvarez Gil, A.; Poggioli, R.; Ruiz, P.; Marttos, A. C.; et al. Umbilical cord mesenchymal stem cells for COVID-19 acute respiratory distress syndrome: A double-blind, phase 1/2a, randomized controlled trial. *Stem Cells Transl. Med.* **2021**, *10* (5), 660−673.

(7) Théry, C.; Witwer, K. W.; Aikawa, E.; Alcaraz, M. J.; Anderson, J. D.; Andriantsitohaina, R.; Antoniou, A.; Arab, T.; Archer, F.; Atkin-Smith, G. K.; et al. Minimal information for studies of extracellular vesicles 2018 (MISEV2018): a position statement of the International Society for Extracellular Vesicles and update of the MISEV2014 guidelines. *J. Extracell. Vesicles* **2018**, *7* (1), 1535750.

(8) Zhu, X.; Badawi, M.; Pomeroy, S.; Sutaria, D. S.; Xie, Z.; Baek, A.; Jiang, J.; Elgamal, O. A.; Mo, X.; La Perle, K.; et al. Comprehensive toxicity and immunogenicity studies reveal minimal effects in mice following sustained dosing of extracellular vesicles derived from HEK293T cells. *J. Extracell. Vesicles* **2017**, *6* (1), 1324730.

(9) Peng, P.; Wang, X.; Qiu, C.; Zheng, W.; Zhang, H. Extracellular vesicles from human umbilical cord mesenchymal stem cells prevent steroid-induced avascular necrosis of the femoral head via the PI3K/AKT pathway. *Food Chem. Toxicol.* **2023**, *180*, 114004.

(10) Lima Correa, B.; El Harane, N.; Gomez, I.; Rachid Hocine, H.; Vilar, J.; Desgres, M.; Bellamy, V.; Keirththana, K.; Guillas, C.; Perotto, M.; et al. Extracellular vesicles from human cardiovascular progenitors trigger a reparative immune response in infarcted hearts. *Cardiovasc. Res.* **2021**, *117* (1), 292−307.

(11) Kadota, T.; Fujita, Y.; Araya, J.; Watanabe, N.; Fujimoto, S.; Kawamoto, H.; Minagawa, S.; Hara, H.; Ohtsuka, T.; Yamamoto, Y.; et al. Human bronchial epithelial cell-derived extracellular vesicle therapy for pulmonary fibrosis via inhibition of TGF-β-WNT crosstalk. *J. Extracell. Vesicles* **2021**, *10* (10), No. e12124.

(12) Tong, L.; Hao, H.; Zhang, Z.; Lv, Y.; Liang, X.; Liu, Q.; Liu, T.; Gong, P.; Zhang, L.; Cao, F.; et al. Milk-derived extracellular vesicles alleviate ulcerative colitis by regulating the gut immunity and reshaping the gut microbiota. *Theranostics* **2021**, *11* (17), 8570−8586.

(13) Redman, C. J. P. Pre-eclampsia and the placenta. *Placenta* **1991**, *12* (4), 301−308.

(14) (a) Matsubara, K.; Matsubara, Y.; Uchikura, Y.; Sugiyama, T. Pathophysiology of Preeclampsia: The Role of Exosomes. *Int. J. Mol. Sci.* **2021**, *22* (5), 2572. (b) Liu, D.; Li, Q.; Ding, H.; Zhao, G.; Wang, Z.; Cao, C.; Dai, Y.; Zheng, M.; Zhu, X.; Wu, Q.; et al. Placenta-derived IL-32β activates neutrophils to promote preeclampsia development. *Cell. Mol. Immunol.* **2021**, *18* (4), 979−991.

(15) (a) Umapathy, A.; Chamley, L. W.; James, J. L. Reconciling the distinct roles of angiogenic/anti-angiogenic factors in the placenta and maternal circulation of normal and pathological pregnancies. *Angiogenesis* **2020**, *23* (2), 105−117. (b) Gebara, N.; Correia, Y.; Wang, K.; Bussolati, B. Angiogenic Properties of Placenta-Derived Extracellular Vesicles in Normal Pregnancy and in Preeclampsia. *Int. J. Mol. Sci.* **2021**, *22* (10), 5402.

(16) Redman, C. W.; Sacks, G. P.; Sargent, I. L. J. A. j. o. o. Preeclampsia: An excessive maternal inflammatory response to pregnancy. *Am J Obstet Gynecol.* **1999**, *180* (2), 499−506.

(17) Roberts, J. M.; Taylor, R. N.; Musci, T. J.; Rodgers, G. M.; Hubel, C. A.; McLaughlin, M. K. Preeclampsia: an endothelial cell disorder. *Am. J. Obstet. Gynecol.* **1989**, *161* (5), 1200−1204.

(18) Lip, S. V.; Boekschoten, M. V.; Hooiveld, G. J.; van Pampus, M. G.; Scherjon, S. A.; Plösch, T.; Faas, M. M. Early-onset preeclampsia, plasma microRNAs, and endothelial cell function. *Am. J. Obstet. Gynecol.* **2020**, *222* (5), 497.e1−497.e12.

(19) Nunes, P. R.; Mattioli, S. V.; Sandrim, V. C. NLRP3 Activation and Its Relationship to Endothelial Dysfunction and Oxidative Stress: Implications for Preeclampsia and Pharmacological Interventions. *Cells* **2021**, *10* (11), 2828.

(20) Opichka, M. A.; Rappelt, M. W.; Gutterman, D. D.; Grobe, J. L.; McIntosh, J. J. Vascular Dysfunction in Preeclampsia. *Cells* **2021**, *10* (11), 3055.

(21) Nunes, P. R.; Bueno Pereira, T. O.; Bertozzi Matheus, M.; Grandini, N. A.; Siqueira, J. S.; Correa, C. R.; Abbade, J. F.; Sandrim, V. C. Glibenclamide Increases Nitric Oxide Levels and Decreases Oxidative Stress in an In Vitro Model of Preeclampsia. *Antioxidants* **2022**, *11* (8), 1620.

(22) Liu, L.; Wang, R.; Xu, R.; Chu, Y.; Gu, W. Procyanidin B2 ameliorates endothelial dysfunction and impaired angiogenesis via the Nrf2/PPARγ/sFlt-1 axis in preeclampsia. *Pharmacol. Res.* **2022**, *177*, 106127.

(23) Gu, S.; Zhou, C.; Pei, J.; Wu, Y.; Wan, S.; Zhao, X.; Hu, J.; Hua, X. Esomeprazole inhibits hypoxia/endothelial dysfunction-induced autophagy in preeclampsia. *Cell Tissue Res.* **2022**, *388* (1), 181−194.

(24) Ives, C. W.; Sinkey, R.; Rajapreyar, I.; Tita, A. T. N.; Oparil, S. Preeclampsia-Pathophysiology and Clinical Presentations: JACC State-of-the-Art Review. *J. Am. Coll. Cardiol.* **2020**, *76* (14), 1690−1702.

(25) Wei, Q.; Wang, Y.; Ma, K.; Li, Q.; Li, B.; Hu, W.; Fu, X.; Zhang, C. Extracellular Vesicles from Human Umbilical Cord Mesenchymal Stem Cells Facilitate Diabetic Wound Healing Through MiR-17−5p-mediated Enhancement of Angiogenesis. *Stem Cell Rev. Rep.* **2022**, *18*, 1025−1040.

(26) (a) Zhu, Y.; Zhang, J.; Hu, X.; Wang, Z.; Wu, S.; Yi, Y. Extracellular vesicles derived from human adipose-derived stem cells promote the exogenous angiogenesis of fat grafts via the let-7/AGO1/VEGF signalling pathway. *Sci. Rep.* **2020**, *10* (1), 5313. (b) Zheng, S.; Shi, A.; Hill, S.; Grant, C.; Kokkinos, M. I.; Murthi, P.; Georgiou, H. M.; Brennecke, S. P.; Kalionis, B. Decidual mesenchymal stem/stromal cell-derived extracellular vesicles ameliorate endothelial cell proliferation, inflammation, and oxidative stress in a cell culture model of preeclampsia. *Pregnancy Hypertens.* **2020**, *22*, 37−46. (c) Xiong, Z. H.; Wei, J.; Lu, M. Q.; Jin, M. Y.; Geng, H. L. Protective effect of human umbilical cord mesenchymal stem cell exosomes on preserving the morphology and angiogenesis of placenta in rats with preeclampsia. *Biomed. Pharmacother.* **2018**, *105*, 1240−1247.

(27) Menichini, D.; Feliciello, L.; Neri, I.; Facchinetti, F. L-Arginine supplementation in pregnancy: a systematic review of maternal and fetal outcomes. *J. Matern. Fetal Neonatal Med.* **2023**, *36* (1), 2217465.

(28) Xiao, S.; Xiao, C.; Miao, Y.; Wang, J.; Chen, R.; Fan, Z.; Hu, Z. Human acellular amniotic membrane incorporating exosomes from adipose-derived mesenchymal stem cells promotes diabetic wound healing. *Stem Cell Res. Ther.* **2021**, *12* (1), 255.

(29) Chinnici, C. M.; Iannolo, G.; Cittadini, E.; Carreca, A. P.; Nascari, D.; Timoneri, F.; Bella, M. D.; Cuscino, N.; Amico, G.; Carcione, C.; et al. Extracellular Vesicle-Derived microRNAs of Human Wharton's Jelly Mesenchymal Stromal Cells May Activate Endogenous VEGF-A to Promote Angiogenesis. *Int. J. Mol. Sci.* **2021**, *22* (4), 2045.

(30) (a) Zullino, S.; Buzzella, F.; Simoncini, T. Nitric oxide and the biology of pregnancy. *Vasc. Pharmacol.* **2018**, *110*, 71−74. (b) Osol, G.; Ko, N. L.; Mandalà, M. Altered Endothelial Nitric Oxide Signaling as a Paradigm for Maternal Vascular Maladaptation in Preeclampsia. *Curr. Hypertens. Rep.* **2017**, *19* (10), 82.

(31) Sutton, E. F.; Gemmel, M.; Powers, R. W. Nitric oxide signaling in pregnancy and preeclampsia. *Nitric Oxide* **2020**, *95*, 55−62.

https://doi.org/10.1021/acs.molpharmaceut.3c00816
Mol. Pharmaceutics 2023, 20, 6429−6440

(32) (a) de Alwis, N.; Binder, N. K.; Beard, S.; Mangwiro, Y. T.; Kadife, E.; Cuffe, J. S.; Keenan, E.; Fato, B. R.; Kaitu'u-Lino, T. J.; Brownfoot, F. C.; et al. The L-NAME mouse model of preeclampsia and impact to long-term maternal cardiovascular health. *Life Sci. Alliance* **2022**, *5* (12), No. e202201517. (b) Yu, Z.; Liu, Y.; Zhang, Y.; Cui, J.; Dong, Y.; Zhang, L.; Liu, P.; Hao, Y.; Xu, Y.; Wang, J. Ulinastatin ameliorates preeclampsia induced by N(gamma)-nitro-l-arginine methyl ester in a rat model via inhibition of the systemic and placental inflammatory response. *J. Hypertens.* **2023**, *41* (1), 150−158. (c) Choi, M.; Hwang, J. R.; Sung, J.-H.; Byun, N.; Seok, Y. S.; Cho, G. J.; Choi, S.-J.; Kim, J.-S.; Oh, S.-Y.; Roh, C.-R. Hydroxychloroquine reduces hypertension and soluble fms-like kinase-1 in a Nω-nitro-l-arginine methyl ester-induced preeclampsia rat model. *J. Hypertens.* **2022**, *40* (12), 2459−2468.

(33) Guerby, P.; Tasta, O.; Swiader, A.; Pont, F.; Bujold, E.; Parant, O.; Vayssiere, C.; Salvayre, R.; Negre-Salvayre, A. Role of oxidative stress in the dysfunction of the placental endothelial nitric oxide synthase in preeclampsia. *Redox Biol.* **2021**, *40*, 101861.

(34) Németh, B.; Murányi, E.; Hegyi, P.; Mátrai, P.; Szakács, Z.; Varjú, P.; Hamvas, S.; Tinusz, B.; Budán, F.; Czimmer, J.; et al. Asymmetric dimethylarginine levels in preeclampsia - Systematic review and meta-analysis. *Placenta* **2018**, *69*, 57−63.

(35) Guerby, P.; Swiader, A.; Augé, N.; Parant, O.; Vayssière, C.; Uchida, K.; Salvayre, R.; Negre-Salvayre, A. High glutathionylation of placental endothelial nitric oxide synthase in preeclampsia. *Redox Biol.* **2019**, *22*, 101126.

(36) Guerby, P.; Swiader, A.; Tasta, O.; Pont, F.; Rodriguez, F.; Parant, O.; Vayssière, C.; Shibata, T.; Uchida, K.; Salvayre, R.; et al. Modification of endothelial nitric oxide synthase by 4-oxo-2(E)-nonenal(ONE) in preeclamptic placentas. *Free Radic. Biol. Med.* **2019**, *141*, 416−425.

https://doi.org/10.1021/acs.molpharmaceut.3c00816
Mol. Pharmaceutics 2023, 20, 6429−6440